Novel Preamble Design for Channel Estimation in FBMC/OQAM Systems

Han Wang[1], Wencai Du[1*] and Lingwei Xu[2]
[1] College of Information Science & Technology, Hainan University
Haikou, Hainan 570228 - China
[e-mail: hanwang1214@gmail.com, wencai@hainu.edu.cn]
[2] Department of Information Science & Engineering, Qingdao University of Science & Technology
Qingdao, Shandong 266061 - China
[e-mail: gaomilaojia2009@163.com]
*Corresponding author: Wencai Du

Received December 20, 2015; revised May 20, 2016; revised June 25, 2016; accepted July 3, 2016; published August 31, 2016

Abstract

The nonorthogonality between the real and imaginary FBMC/OQAM modulated signals complicates the channel estimation (CE) process, and conventional OFDM CE methods cannot be directly applied to FBMC/OQAM. The conventional preamble-based CE schemes in FBMC/OQAM systems are mainly based on the interference approximation method (IAM) to improve the estimation performance. In this paper, we develop a novel preamble structure to improve the CE performance. We exploit the symmetry pattern to cancel interference and take into account the interference weights in this symmetric structure. The conventional preamble and the proposed preamble are compared via simulations in the IEEE 802.22, 3GPP Vehicular A and Pedestrian A channels. Numerical simulation results demonstrate that the proposed preamble can achieve better bit error ratio (BER) and mean squared error (MSE) performance under the three channel models considered.

Keywords: FBMC/OQAM, channel estimation, preamble, BER, MSE

This research was supported by the National Natural Science Foundation of China (Grant No.61561017, No.61561018). We express our thanks to the editor and the anonymous reviewers for their valuable comments.

http://dx.doi.org/10.3837/tiis.2016.08.014 **ISSN : 1976-7277**

1. Introduction

Multicarrier communication techniques have been widely adopted in recent years for high data rate transmission. Cyclic prefix-based orthogonal frequency division multiplexing (CP-OFDM) is certainly the most researched and accepted multicarrier technology among the various wireless communications standards [1-3]. With the insertion of some redundancy, the frequency selective channel becomes a frequency flat subchannel. However, the disadvantage of CP-OFDM is a loss in spectral efficiency due to the CP insertion, and a higher sensitivity to narrowband interferers and Doppler spread. As described in Ref. [4], up to 25% transmitted power as well as spectral efficiency is wasted because of the inclusion of CP.

Unlike the CP-OFDM system, FBMC/OQAM well utilizes time frequency localization (TFL) property pulse shaping via an IFFT/FFT-based filter bank, and staggered OQAM symbols, real symbols at twice the symbol rate of FBMC/QAM, are loaded on the subcarriers [5]. Hence, FBMC/OQAM has a theoretically higher spectral efficiency [6,7] and increased robustness to frequency offset and Doppler spread. Moreover, CP is not required in FBMC/OQAM systems, which may lead to even higher transmission rates [8]. Moreover FBMC/OQAM has already been introduced into the TIA's digital radio technical standards [9].

FBMC/OQAM has its root in the pioneering works of Chang [10] and Saltzberg [11], who introduced multicarrier techniques over two decades ago. Among the various pulse shaping prototype filters with good TEL properties that have been proposed [12-15], FBMC/OQAM has garnered wide attention and has been the focus of extensive research [16-19]. Because of the subcarrier functions, which are only orthogonal in the real field, there always exist imaginary valued intrinsic interference from neighbor symbols. That is why conventional OFDM CE methods cannot be directly applied to FBMC/OQAM.

A number of FBMC/OQAM CE methods have been recently studied for preamble-based and scattered pilot-based training schemes. A pseudo pilot-based CE method has been proposed in Ref. [20], and a preamble-based CE interference approximation method (IAM) has been proposed in Refs. [21-23]; the IAM schemes include IAM-R, IMA-I, IAM-C, and E-IAM-C, and all of these methods can be characterized as aiming at constructively exploiting interference to improve estimation performance. Extended IAM-C (E-IAM-C) [23] has been identified as the best performance gain in all of the proposed IAM preamble structure schemes so far. In contrast to the IAM approach, in which the interference is taken advantage of to improve CE accuracy, the interference cancellation (IC) approach is designed to cancel or avoid the interference. Such a preamble design has been proposed in Refs. [24-27], and a more spectral efficiency preamble design method has been suggested in Ref. [28].

In this paper, we investigate the possible maximum gain from existing preamble structures. The major contributions of this paper are as follows:

1. The conventional IAM and IC preamble-based channel estimation methods for FBMC/OQAM are reviewed.

2. A novel preamble structure for channel estimation in FBMC/OQAM system is proposed.

3. The proposed preamble structure exploits the symmetry pattern to obtain interference cancellation gain and jointly considers the interference weights to obtain a greater interference approximation gain. The idea of the proposed preamble structure is based on a trade-off between IAM and IC, and is called the novel preamble structure (NPS).

4. The superiority of the proposed preamble structure is verified by numerical simulations over IEEE 802.22, 3GPP Vehicular A and Pedestrian A channels.

The rest of this paper is organized as follows: In Sec. 2, we describe the discrete-time baseband equivalent model for FBMC/OQAM systems. In Sec. 3, we review the IAM and IC preamble structures and design the novel preamble structure. The BER and MSE performance of the proposed preamble associated with the conventional preamble-based CE are compared and simulation results for the three aforementioned channel scenarios are presented in Sec. 4. Section 5 concludes the paper.

2. System Model

The transmitted signal in FBMC/OQAM systems can be written in the following form [21]:

$$s(t)=\sum_{m=0}^{N-1}\sum_{n} d_{m,n}g_{m,n}(t) \tag{1}$$

where $d_{m,n}$ are real valued OQAM symbols, and $g_{m,n}(t)$ represents the synthesis basis which is obtained by the time-frequency translated version of the prototype function $g(t)$ in the following way

$$g_{m,n}(t)=g(t-n\tau_0)e^{i2\pi mF_0 t}e^{j\phi_{m,n}} \tag{2}$$

with N an even number of subcarriers, $F_0=1/T_0=1/2\tau_0$ the subcarrie spacing, and $\phi_{m,n}$ an additional phase term. T_0 denotes the OFDM symbol duration, and τ_0 denotes the time offset between the real and imaginary parts of the OQAM symbols. The double subscript $(.)_{m,n}$ denotes the (m,n)-th frequency-time (FT) point, m is the subcarrier index and n is the OQAM symbol time index. **Fig. 1** shows the FBMC/OQAM lattice. For ease of understanding, the OFDM lattice is also shown in **Fig. 1**.

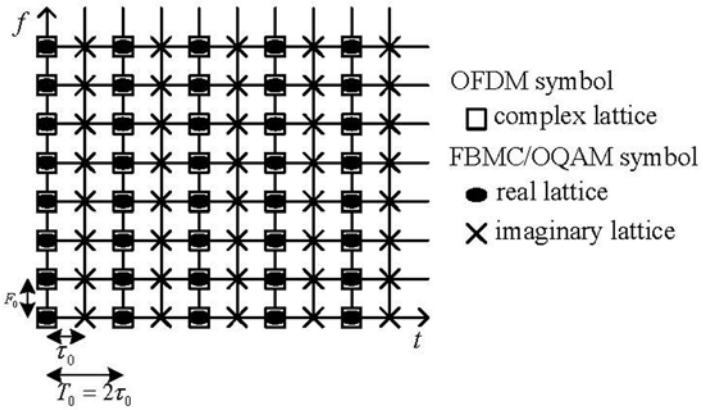

Fig. 1. FBMC/OQAM and OFDM lattices [24].

The pulse g is designed so that the associated subcarrier functions $g_{m,n}$ are orthogonal in the real field, that is

$$\Re\{\left\langle g_{m,n} \middle| g_{p,q} \right\rangle\} = \Re\{\sum_{t} g_{m,n}(t) g^{*}_{p,q}(t)\} = \delta_{m,p}\delta_{n,q} \tag{3}$$

where $\delta_{i,j}$ is the Kronecker delta, $\delta_{m,p} = 1$ if $m = p$ and $\delta_{m,p} = 0$ if $m \neq p$. We can find that even in the distortion-free channel and with perfect time and frequency synchronization, there still will be some purely imaginary intercarrier interference at the output; thus, we set interference weights

$$\left\langle g \right\rangle_{m,n}^{p,q} = -j \left\langle g_{m,n} \middle| g_{p,q} \right\rangle \tag{4}$$

with $\left\langle g_{m,n} \middle| g_{p,q} \right\rangle$ a purely imaginary term for $(m,n) \neq (p,q)$.

After passing through the channel, the received signal with an additive noise can be written as

$$r(t) = \sum_{m=0}^{M-1} \sum_{n} d_{m,n} g_{m,n}(t) H_{m,n}(t) + \eta(t) \tag{5}$$

with

$$H_{m,n}(t) = \int_{0}^{\tau_{\max}} h(t,\tau) e^{-2j\pi m F_0 \tau} d\tau \tag{6}$$

where $h(t,\tau)$ is the channel impulse response. $H_{m,n}(t)$ is the complex response of the channel at instant t. We assume that we have a flat fading channel at each subcarrier, which means that the channel is constant during the duration of the prototype, then $H_{m,n}(t) = H_{m,n}$. **Fig. 2** shows the implementation diagram of the FBMC/OQAM system, which was proposed by Jinfeng Du and Svante Signell [5].

When the output is at the p-th subcarrier and q-th OQAM symbol, the output signal, with the noise separated out, can be expressed as

$$\begin{aligned} y_{p,q} &= \left\langle r \middle| g_{p,q} \right\rangle \\ y_{p,q} &= H_{p,q} d_{p,q} + j \sum_{(m,n)\neq(0,0)} d_{p+m,q+n} H_{p+m,q+n} \left\langle g \right\rangle_{p+m,q+n}^{p,q} \end{aligned} \tag{7}$$

A common definition is that only the first-order neighborhood $\Omega_{1,1}$ of a given FT point (p,q), $\Omega_{1,1} = \{(m,n), |m| \leq 1, |n| \leq 1, (m,n) \neq (0,0)\}$, causes the interference, and assuming that the channel is almost constant over this neighborhood, we can rewrite (7) as

$$\begin{aligned} y_{p,q} = H_{p,q} d_{p,q} &+ j \sum_{(m,n)\in\Omega_{1,1}} H_{p,q} d_{p+m,q+n} \left\langle g \right\rangle_{p+m,q+n}^{p,q} \\ &+ j \sum_{(m,n)\notin\Omega_{1,1}} \frac{H_{p+m,q+n}}{H_{p,q}} d_{p+m,q+n} \left\langle g \right\rangle_{p+m,q+n}^{p,q} \end{aligned} \tag{8}$$

with the increase of m and n, and $\langle g \rangle_{p+m,q+n}^{p,q}$ becomes very close to zero [5]; (8) can then be rewritten as

$$y_{p,q} \approx H_{p,q} d_{p,q} + j \sum_{(m,n)\in\Omega_{1,1}} H_{p,q} d_{p+m,q+n} \langle g \rangle_{p+m,q+n}^{p,q} \tag{9}$$

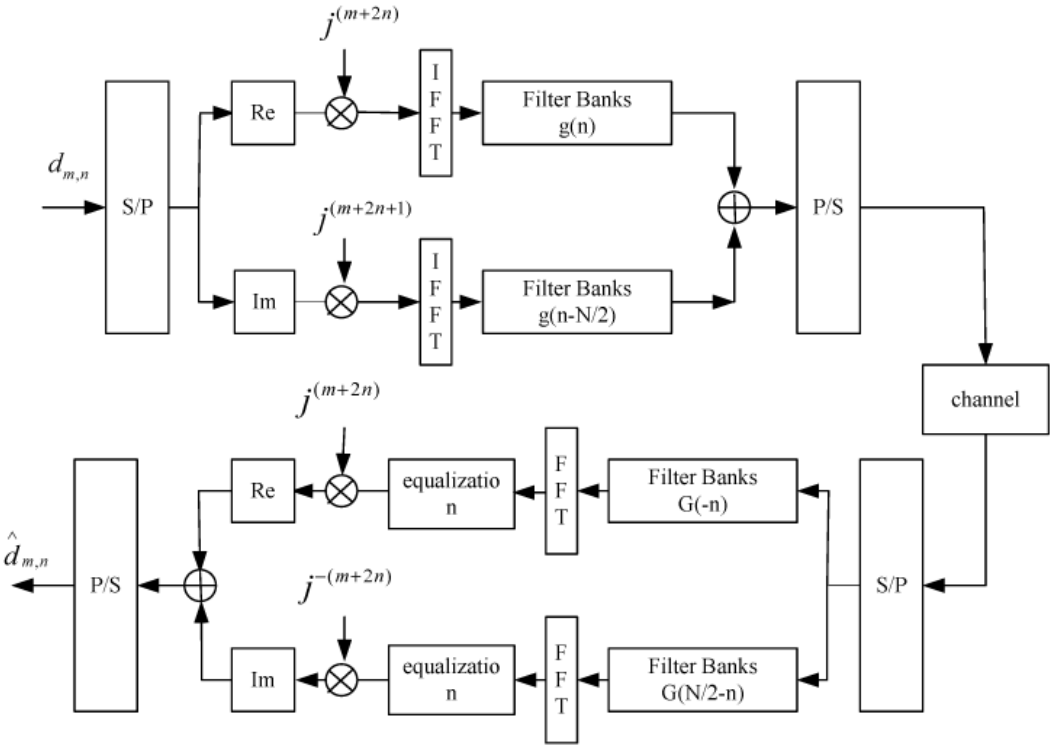

Fig. 2. Implementation diagram of the FBMC/OQAM system [5].

The zero-forcing (ZF) equalized signal can be written as

$$\frac{y_{p,q}}{H_{p,q}} == d_{p,q} + j \underbrace{\sum_{(m,n)\in\Omega_{1,1}} d_{p+m,q+n} \langle g \rangle_{p+m,q+n}^{p,q}}_{d_{p,q}^{i}} \tag{10}$$

As $\sum_{(m,n)\in\Omega_{1,1}} d_{p+m,q+n} \langle g \rangle_{p+m,q+n}^{p,q}$ is a pure real term, the estimated symbol is given by

$$\hat{d}_{p,q} = \Re\left\{\frac{y_{p,q}}{H_{p,q}}\right\} \approx d_{p,q} \tag{11}$$

From (11), we can infer that the inter symbol interference (ISI) can be neglected, in practice, with prototype functions well localized in both time and frequency.

Considering Gaussian noise η with zero mean and variance σ^2, the CE formula can be expressed as

$$\hat{H}_{p,q} = H_{p,q} + \frac{\eta}{d_{p,q} + jd^{i}_{p,q}} \tag{12}$$

Note that the larger the power of $d_{p,q} + jd^{i}_{p,q}$, the better the CE will be. This observation underlies the IAM schemes, which will be discussed in the following section.

3. Preamble-based Channel Estimation Methods

Since our focus in this paper is on preamble-based channel estimation in FBMC/OQAM systems, in this section we review the IAM and IC approaches and propose the novel preamble structure.

3.1 Interference Approximation Method (IAM)

The first-order neighborhood is considered, and the preamble length is taken equal to $3\tau_0$ and is assumed to be perfectly known at the receiver. $d_{p,q}$ is located in the middle of the preamble. As introduced in formula (12), the symbols surrounding $d_{p,q}$ should have the same sign so that they can be added together; then, the greater the power of $d_{p,q} + jd^{i}_{p,q}$, the better the estimation will be.

We should also know the interference weights $\langle g \rangle^{p,q}_{m,n}$ for neighbors $(m,n) \in \Omega_{p,q}$ of each FT point (p,q). The values can be computed based on the prototype filter g, and thus, for all q, the interference weights are given by

$$\begin{array}{ccc} (-1)^p \varepsilon & 0 & -(-1)^p \varepsilon \\ (-1)^p \delta & -\beta & (-1)^p \delta \\ -(-1)^p \gamma & \mathrm{d}_{p,q} & (-1)^p \gamma \\ (-1)^p \delta & \beta & (-1)^p \delta \\ (-1)^p \varepsilon & 0 & -(-1)^p \varepsilon \end{array} \tag{13}$$

Details can be found in Ref. [23]. Generally, $\beta, \gamma > \delta$. The above quantities can be given by

$$\beta = e^{-j\frac{2\pi}{N}\frac{L-1}{2}} \sum_{l=0}^{L-1} g^2(l) e^{j\frac{2\pi}{N}l} \tag{14}$$

$$\gamma = \sum_{l=\frac{N}{2}}^{L-1} g(l) g(l - \frac{N}{2}) \tag{15}$$

$$\delta = -je^{-j\frac{2\pi}{N}\frac{L-1}{2}} \sum_{l=N/2}^{L-1} g(l) g(l - \frac{N}{2}) e^{j\frac{2\pi}{N}l} \tag{16}$$

$$\varepsilon = e^{\mp j\frac{2\pi}{N}(L-1)} \sum_{l=N/2}^{L-1} g(l)g(l-\frac{N}{2})e^{\mp j2\frac{2\pi}{N}l} \tag{17}$$

In Sec. 4, $\gamma = 0.5004$, β=0.3183, δ=0.2501, and $\varepsilon = 0$ for the design of g.

In order to simplify the maximum preamble magnitude problem, IAM-R was proposed in Ref. [21] to place nulls at the first and third FBMC/OQAM symbols of the preamble,

where $d_{p,0} = d_{p,2} = 0$, $\mathrm{d}_{p+1,1} = -\mathrm{d}_{p-1,1}$, p=0,1,2...,N-1, we assume $\left|d_{p,1}\right|^2 = d^2$, and then the power of $d_{p,q} + jd_{p,q}^i$ can be expressed as

$$\begin{aligned} &E\left\{\left|d_{p,1} + j(d_{p+1,1}\langle g\rangle_{p+1,1}^{p,1} + d_{p-1,1}\langle g\rangle_{p-1,1}^{p,1})\right|^2\right\} \\ &= E\left\{d^2\left|1+j2\beta\right|^2\right\} = d^2(1+4\beta^2) \end{aligned} \tag{18}$$

Fig. 3(a) shows an example with $N = 8$, for OQAM modulation of the IAM-R preamble structure.

Furthermore, one may try to find a complex valued preamble sequence so that the power of $d_{p,q} + jd_{p,q}^i$ will be maximized. With a slight modification, the pilot symbols are either purely real or imaginary at all the subcarriers. This operation is to set the middle FBMC/OQAM symbol equal to that in IAM-R, but with pilots at the odd subcarriers multiplied by j. This preamble structure, proposed in Ref. [28], is called IAM-C. The power of $d_{p,q} + jd_{p,q}^i$ is $E\left\{d^2\left|1+2\beta\right|^2\right\} = d^2(1+4\beta+4\beta^2)$. Obviously, the power of $d_{p,q} + jd_{p,q}^i$ in IAM-C is larger than that achieved by IAM-R. **Fig. 3(b)** shows the IAM-C preamble structure, for $N = 8$, and OQAM modulation.

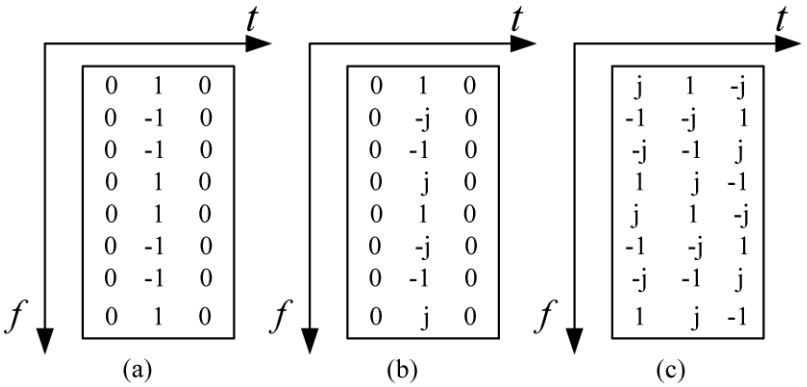

Fig. 3. Preamble structures for (a) IAM-R, (b) IAM-C, and (c) E-IAM-C.

In IAM-C, nulls are placed in the first and third symbol positions, and thus one may think to utilize the first and third symbols to obtain the maximum possible power of the preamble. Considering the analysis of presented at the end of Sec. 2, an alternative preamble structure that employs the side symbols as well could yield pilots that are stronger than those of IAM-C.

A method based on this idea, proposed in Ref. [23], is called extended IAM-C (E-IAM-C). The preamble magnitude is $d\left|1+2(\beta+\gamma)\right|$; clearly, the power of $d_{p,q}+jd_{p,q}^{i}$ is larger than that achieved by IAM-C. An example of E-IAM-C is given in **Fig. 3(c).**

3.2 Interference Cancellation (IC) Method

In IAM schemes, inter-pilot interference is removed by an opposite sign between adjacent subcarriers in the frequency domain and inter symbol interference is prevented by an insertion of nulls. An alternative approach is presented to cancel or avoid the intrinsic interference, and is called the interference cancellation (IC) method.

A straightforward way to cancel the interference is to simply null the data surrounding the pilot FT point. IAM-R is considered to be a special IC method. Another way to simplify the interference cancellation is to transmit zeros at the middle symbol, at all odd indexed subcarriers. Such a preamble was proposed in Ref. [27]. Another design, which relies on the symmetries in (13) to cancel the interference from adjacent subcarriers, was suggested in Ref. [24]. Like the idea of E-IAM-C, the neighborhood symbols utilize the symmetries to transmit data at the FT positions instead of nulls [28], which was confirmed to have the better CE performance among interference cancellation methods. Following the pattern in (13), the data modulating the first order neighbors could be structured as

$$\begin{matrix} a & \mathrm{b} & c \\ d & \mathrm{s} & d \\ -a & \mathrm{b} & -c \end{matrix} \tag{19}$$

One can use the above structure to design a preamble with the property of interference cancellation by simply applying the pattern for every third subcarrier and resorting to interpolation for the rest. This makes it true that the interference weights are the same for every second subcarrier. **Fig. 4** depicts some examples of IC preamble structures, with $N=8$, and OQAM modulation.

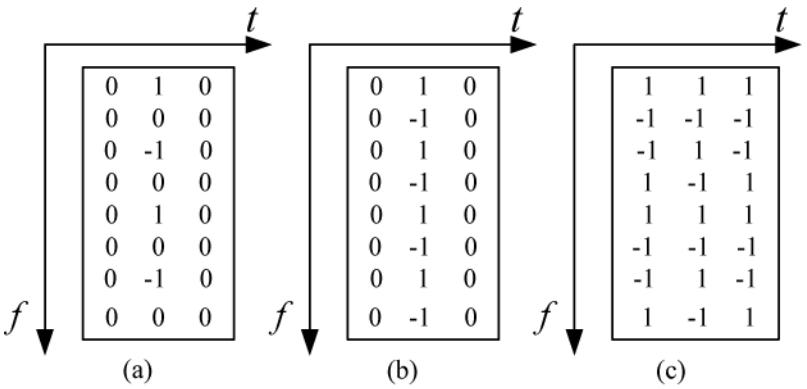

Fig. 4. Preamble structures for IC methods from (a) Ref. [27], (b) Ref. [24], and (c) Ref. [28].

3.3 Novel Preamble Structure (NPS)

It was shown in Ref. [28] that the preamble structure could have better CE performance in IC methods. However, in contrast with the IAM approach, this method is only considered to cancel the neighborhood interference, and the influence of interference power on CE

performance is ignored.

We see in **Fig. 4(c)** that the interference cancellation is reflected in all subcarriers. The structure with magnitude d is clearly smaller than in IAM approaches. However, simulation results [28] show that, compared to IAM approaches, this preamble-based CE method can achieve better BER and MSE performance.

Based on the idea of maximum interference cancellation gain from all the subcarriers and the larger power of $d_{p,q} + jd_{p,q}^{i}$, we consider every fourth subcarrier to be modulated, and propose a novel preamble structure. The proposed structure is using symmetry pattern to combine both interference cancellation gaindan interference approximation gain.

In the following equation, we consider the preamble pairs $S_{i,j}$ $(i = 0,1, j = 0,1)$ which cancel each other in order to remove interference at the pilot location:

$$\begin{array}{ccc} S_{-1,1} & S_{0,1} & S_{1,1} \\ S_{-1,0} & \text{pilot} & S_{1,0} \\ S_{-1,-1} & S_{0,-1} & S_{1,-1} \end{array} \tag{20}$$

At an odd-indexed subcarrier, the pilot $\pm d$ in the middle, $\begin{cases} S_{i,1} = -S_{i,-1} & (j = 1, \text{expect } S_{-1,1} = S_{-1,-1}) \\ S_{i,0} = S_{-i,0} & (j = 0) \end{cases}$. At an even-indexed sub-carrier, with the pilot d in the middle, $\begin{cases} S_{i,1} = -S_{i,-1} & (j = 1) \\ S_{i,0} = -S_{-i,0} & (j = 0) \end{cases}$, and with the pilot $-d$ in the middle, $\begin{cases} S_{i,1} = -S_{i,-1} & (j = 1) \\ S_{i,0} = S_{-i,0} & (j = 0) \end{cases}$.

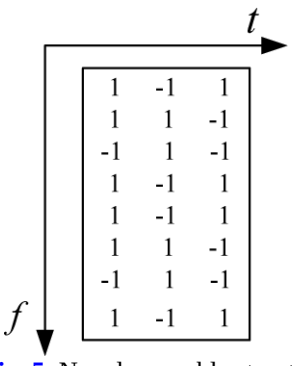

Fig. 5. Novel preamble structure.

An example is given, at an odd-indexed subcarrier, with the pilots $\mp d$ in the middle, and $\pm d$ placed at the right and left neighborhood positions. When at an even-indexed subcarrier, the middle pilots are $\pm d$, with d placed at the right neighborhood position, and its negative, $\mp d$ placed at the left neighborhood position. Then from calculations, at an odd-indexed subcarrier, when the middle pilot is d, the preamble has magnitude $d\left|1 - j2(\beta + \delta)\right|$, and

when the middle pilot is $-d$, the preamble has magnitude $d\left|1-j2\left(\delta-\beta\right)\right|$; where $\beta>\delta$, obviously, the magnitude is larger than d . At an even-indexed subcarrier, with the pilot d in the middle, the preamble has magnitude $d\left|1+j2\left(\beta-\gamma\right)\right|$, and with the pilot $-d$ in the middle, the preamble has magnitude $d\left|1+j2\beta\right|$. It is clear that in a pair of subcarrier pilots, one of its magnitudes is larger than that achieved by conventional interference cancellation. Compared to IAM approaches, the proposed structure has a smaller magnitude, but takes into account interference cancellation. Furthermore, the proposed structure has a larger magnitude than conventional IC approaches. **Fig. 5** gives an example of an NPS, with $N=8$, and OQAM modulation.

4. Simulation Results

In this section, we present simulation results to verify our analysis, and the BER and MSE performance of the two conventional preamble schemes (IAM and IC) versus the proposed preamble scheme are discussed. There have been many previous studies [29-31] of CP-OFDM and FBMC/OQAM that have concluded that an FBMC/OQAM system for preamble-based CE obtains better performance than a CP-OFDM system, so our simulation analysis will not include a CP-OFDM system.

The simulations were carried out with three channel models and modulation parameters. The channel models are the IEEE 802.22 A, 3GPP Vehicular A and Pedestrian A channels. The IEEE 802.22 standard aims at constructing wireless regional area network (WRAN) utilizing free TV bands. 3GPP two channel models provide different delay path parameters. Main parameters are inspired from the IEEE 802.22 standard [1]. The three channel profiles and main parameters of the system used are shown in **Tables 1** and **2.**

Table 1. Profiles of the three channels.

IEEE 802.22 A channel	Path 1	Path 2	Path 3	Path 4	Path 5	Path 6
Delay (μs **)**	0	3	8	11	13	21
Relative power(dB **)**	0	-7	-15	-22	-24	-19
3GPP Vehicular A channel	Path 1	Path 2	Path 3	Path 4	Path 5	Path 6
Delay (ns **)**	0	310	710	1090	1730	2510
Relative power(dB **)**	0	-1	-9	-10	-15	-20
3GPP Pedestrian A channel	Path1	Path 2	Path 3	Path 4		
Delay (ns **)**	0	110	190	410		
Relative power(dB **)**	0	-9.7	-19.2	-22.8		

Table 2. Main parameters of the systems.

Simulation channels	IEEE 802.22 A channel/3GPP Vehicular A channel/3GPP Pedestrian A channel
Sampling frequency	6.86 MHz/10 MHz/10 MHz
FFT/IFFT size	2048
Channel coding	Convolutional code ($K=7$, with $g_1=(133)_o$, $g_2=(171)_o$ and code rate=1/2)
Frame length	40 OFDM symbols

We utilize prototype filters of finite length, denoted by L, that are well-localized in time and frequency. The prototype filter is obtained from the isotropic orthogonal transform algorithm (IOTA), the design of which is described in Ref. [12]. The truncation of the IOTA prototype function, limiting its duration to $4T_0$, contains $L = 4N = 8192$ taps. The bit error ratio (BER) is the number of bit errors divided by the total number of transferred bits during a studied time interval. The MSE, $\frac{1}{N}\sum_{m=0}^{N}\frac{\left|H_m - \hat{H}_m\right|^2}{\left|H_m\right|^2}$, where H_m is the m th subcarrier channel value, and $\hat{H}_m$ its estimated value, is plotted with respect to the signal-to-noise ratio (SNR).

Figs. 6(a) and (b) show the BER and MSE performance of the proposed preamble and conventional preambles in the IEEE 802.22 channel model. It is obvious that, in both the BER and MSE cases, the NPS outperforms the other preamble schemes over the entire SNR range considered. In **Fig. 6(a)**, we see that the NPS is slightly better performing than the IC in Ref. [28] method, but has a gain of about 1 and 3 dB compared to E-IAM-C and IAM-C, respectively, when a BER of 10^{-2} is considered. IC in the scheme described in Ref. [28] outperforms IC the scheme described in Ref. [27] scheme over the entire SNR range considered. The E-IAM-C method performs slightly better than the IC method described in Ref. [27] for low to moderate SNR values. At higher SNRs, the IC method described in Ref. [27] exhibits the better performance, while the BER curves of the E-IAM-C scheme exhibit an error floor. This phenomenon in FBMC/OQAM is due to the fact that the approximation is not exact for channels with significant time dispersion. The trend of the NPS curve may be due to the fact that the value of $d_{p,q} + jd_{p,q}^{i}$ is variable in odd and even subcarrier, as the analysis described in Sec. 3 shows, its value is greater than that in the IC method at half of the probability, and the other half is less than that.

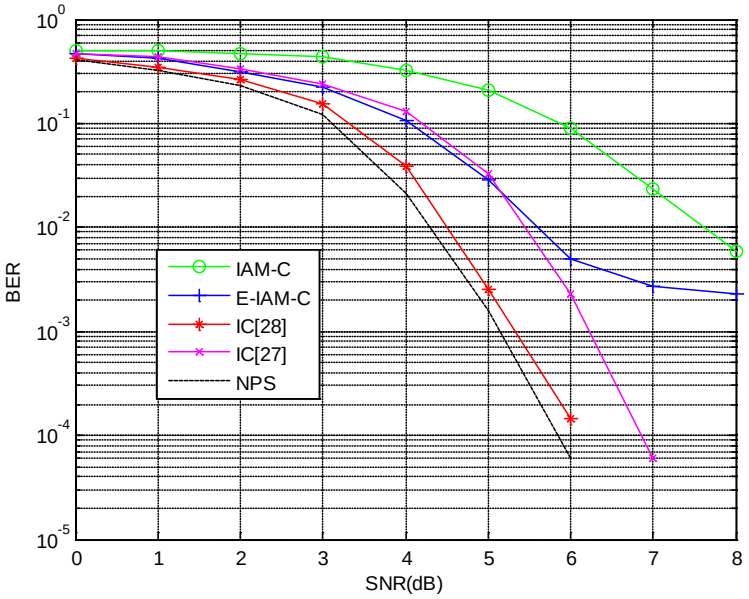

(a)

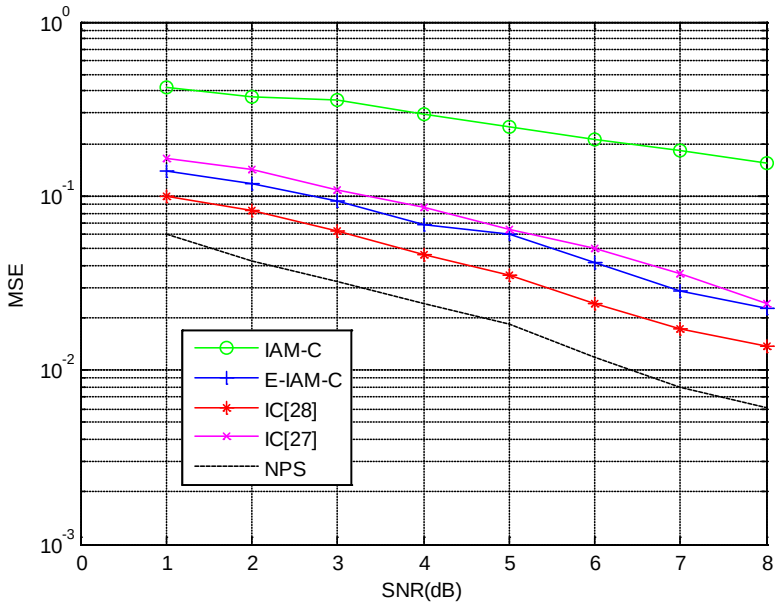

(b)

Fig. 6. (a) BER and (b) MSE performance of the proposed preamble and conventional preambles in the IEEE 802.22 channel.

It can be seen from **Fig. 6(b)** that, compared with the conventional IC and IAM methods, the channel estimation is effectively improved by the proposed NPS method. The reason is that the variance of $\frac{\eta}{d_{p,q} + jd_{p,q}^{i}}$ is reduced with the NPS method, which improves the channel estimation accuracy. The NPS method provides a significant SNR gain compared to those of the Ref. [27] IC, Ref. [28] IC, IAM-C and E-IAM-C methods at the same MSE level.

Figs. 7(a) and (b) depict the performance of the preambles under the Vehicular A channel, which has a higher sampling frequency than the IEEE 802.22 model as shown in **Table 2**. Results show an improved performance of the NPS compared to the other four methods, for both BER and MSE measurements.

From **Fig. 7(a)**, compared to the IC and IAM methods, the BER performance is improved with the proposed NPS method. When BER=10^{-2}, the NPS gives performances that are approximately 0.2 dB better than the Ref. [28] IC method, and 1.2, 1.6 and 3.2 dB better than the Ref. [27] IC, E-IAM-C and IAM-C, respectively. The performances for the schemes get very close to each other, because we have adopted a higher sampling frequency channel model. From **Fig. 7(b)**, compared with the conventional four methods, the channel estimation is effectively improved by the NPS. We can find that the MSE performance gains of the NPS scheme compared to the other schemes are evidently less than that shown in **Fig. 6(b)**. The MSE performance of the proposed scheme is 2, 4 and 3.7 dB better than that of the Ref. [28] IC, Ref. [27] IC and E-IAM-C schemes, respectively, when the target MSE of 10^{-2} is considered. The IAM-C scheme cannot work due to the limiting effect of the SNR region, and its MSE performance is still the worst.

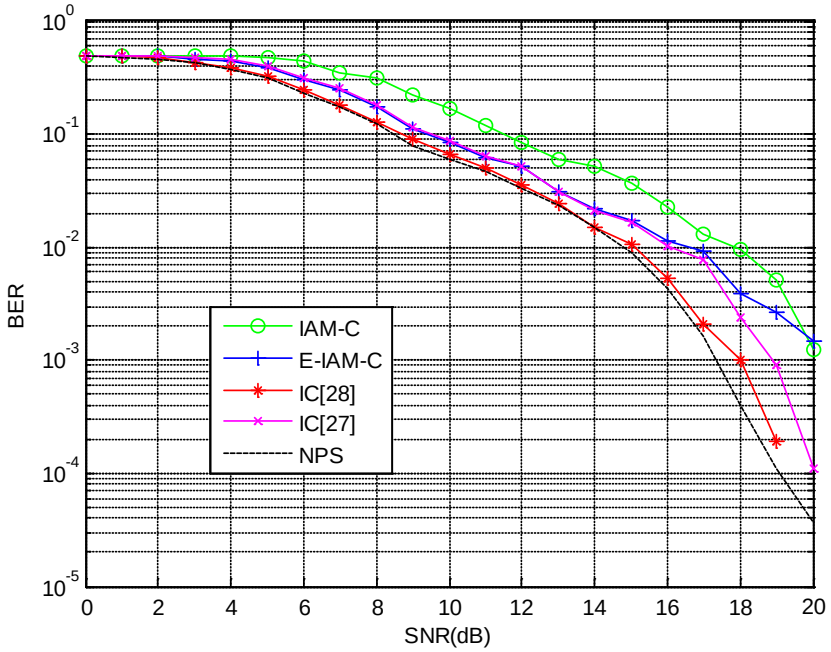

(a)

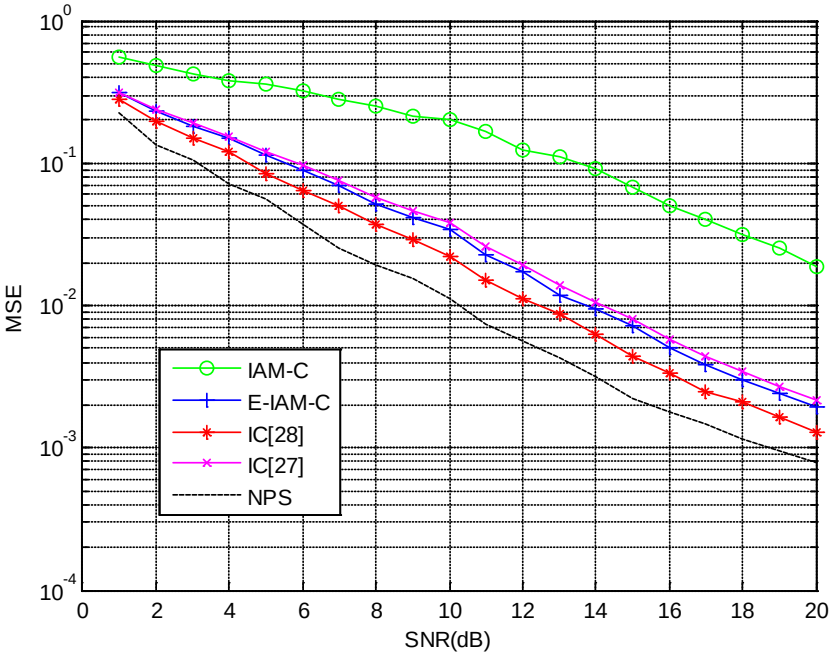

(b)

Fig. 7. (a) BER and (b) MSE performance of the proposed preamble and conventional preambles in the Vehicular A channel.

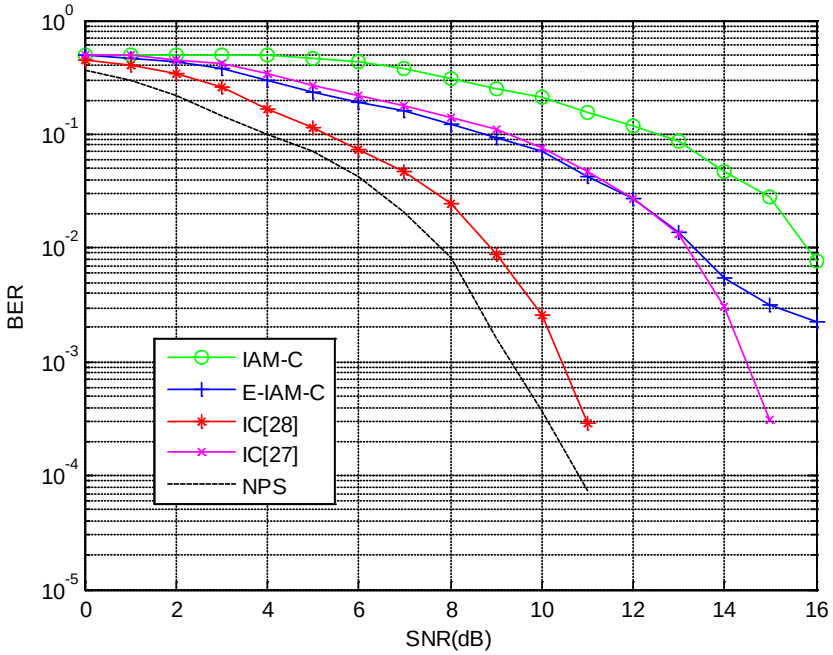

(a)

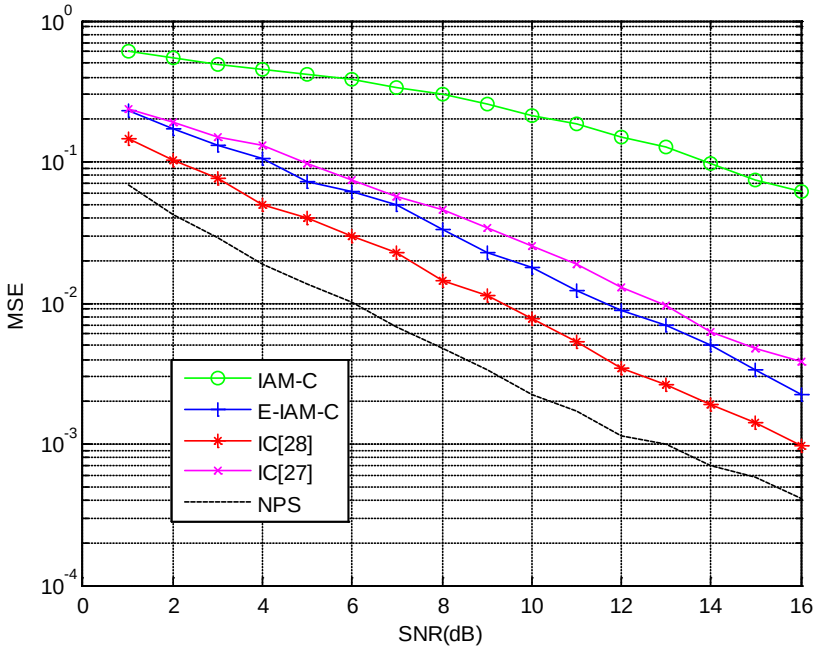

(b)

Fig. 8. (a) BER and (b) MSE performance of the proposed preamble and conventional preambles in the Pedestrian A channel.

The Pedestrian A-type channel is considered in **Figs. 8(a) and (b)**, where it is shown that the NPS provides effective channel estimation performance improvement that is greater than the other four methods. Reducing the number of delay paths to four, it can be observed from **Fig. 8(a)** that the entire BER performance is better than that shown in **Fig. 7(a)**, but worse than that shown in **Fig. 6(a)**. The interval between the NPS and IC curves is wider than in **Figs. 6(a)** and **7(a)**. As shown in **Fig. 8(b)**, the MSE performance of the proposed scheme is about 3, 7 and 5.5 dB better than that of the Ref. [28] IC, Ref. [27] IC and E-IAM-C schemes, respectively, when the target MSE of 10^{-2} is considered; the IAM-C scheme still cannot work due to the limiting effect of the SNR region.

From the simulation results, it can be verified that the proposed preamble scheme provides performance improvement in the three channel scenarios considered. When under a lower sampling frequency channel, with the same number of delay paths, the superiority is reflected more obviously, with a lower SNR obtaining a smaller BER, and a better MSE. When the channel sample frequency is uniform, the system with fewer delay paths can achieve better BER and MSE performance.

5. Conclusions

In this paper, we have proposed a novel preamble structure for channel estimation in FBMC/OQAM systems. The IAM and IC schemes are reviewed along with their associated preamble structures. The proposed preamble is compared with three other conventional preambles under the IEEE 802.22, 3GPP Vehicular A, and Pedestrian A channels. The superiority of the proposed preamble-based CE is verified through simulations in the three channel scenarios considered. In the case of low sampling frequency and fewer multipaths, the superiority is reflected more significantly.

References

[1] IEEE 802.22 Working Group on Wireless Regional Area Networks. Article (CrossRef Link)

[2] Project IEEE 802.11g Standard for Higher Rate (20+Mbps) Extensions in the 2.4 GHz Band, *IEEE Standard 802.11g, IEEE P802.11-TASK GROUP G*, 2003. Article (CrossRef Link)

[3] A. Ghosh, R. Ratasuk, B. Mondal, N. Mangalvedhe, and T. Thomas, "LTE-advanced: Next-generation wireless broadband technology," *IEEE Wireless Communications*, vol.17, no.3, pp.10-22, June, 2010. Article (CrossRef Link)

[4] J. G. Andrews, A. Ghosh, and R. Muhamed, *Fundamentals of WiMAX: Understanding Broadband Wireless Networking*. Englewood Cliffs, NJ: Prectice-Hall, 2007. Article (CrossRef Link)

[5] J.F. Du, S. Signell, "Time Frequency Localization of Pulse Shaping Filters in OFDM/OQAM Systems," in *Proc. of 6th International Conference of Information, Communications & Signal Processing*, pp.1-5, December 10-13, 2007. Article (CrossRef Link)

[6] X. W. Chen, M. J. Zhao, C. L. Xu, "Preamble-based Channel Estimation Methods with High Spectral Efficiency for Pulse Shaping OFDM/OQAM Systems," in *Proc. of the 6th International Conference on Wireless Communications and Signal Processing*, pp. 1-6, October 23-25, 2014. Article (CrossRef Link)

[7] R. Razavi, P. Xiao, R. Tafazolli, "Information Theoretic Analysis of OFDM/OQAM with Utilized Intrinsic Interference," *IEEE Signal Processing Letters*, vol. 22, no. 5, pp. 618-622, October, 2015. Article (CrossRef Link)

[8] P. Siohan, C. Siclet, and N. Lacaille, "Analysis and design of OFDM/OQAM systems based on filterbank theory," *IEEE Transactions on Signal Process*, vol. 50, no. 5, pp.1170-1183, May, 2002. Article (CrossRef Link)

[9] TIA Committer TR-8.5, "Wideband Air Interface Isotropic Orthogonal Transform Algorithm (IOTA) Public Safety Wideband Data Standards Project-Digital Radio Technical Standards," 2003. Article (CrossRef Link)
[10] R. Chang, "Synthesis of Band-limited Orthogonal Signals for Multichannel data transmission," *Bell System Technical Journal*, vol. 45, no. 10, pp.1775-1796, 1966. Article (CrossRef Link)
[11] B. Saltzberg, "Performance of an efficient parallel data transmission system," *IEEE Transactions on Communication Technology*, vol.15, no. 6, pp.805-811, June, 1967. Article (CrossRef Link)
[12] M. G. Bellanger, "Specification and design of a prototype filter for filter bank based multicarrier transmission," in *Proc. of IEEE International Conference on Acoustics, Speech, and Signal Processing*, pp.2417-2420, May 7-11, 2001. Article (CrossRef Link)
[13] M. Al-Attraqchi, S. Boussakta, "An Enhanced OFDM/OQAM System Exploiting Walsh-Hadamard Transform," in *Proc. of the 73rd IEEE Vehicular Technology Conference*, pp.1-5, May 15-18, 2011. Article (CrossRef Link)
[14] M. J. Abdoli, M. Jia, J. L. Ma, "Weighted Circularly Convolved Filtering in OFDM/OQAM," in *Proc. of the 24th IEEE International Symposium on Personal, Indoor and Mobile Radio Communications: Fundamentals and PHY Track*, pp. 657-661, September 8-11, 2013. Article (CrossRef Link)
[15] S. Dashiti, S. M. Fakhraie, "Analysis and design of OFDM/OQAM System with Hexagonal Lattice Based on Filter bank Theory," in *Proc. of the 7th International Symposium on Telecommunications (IST2014)*, pp. 383-387, September 9-11, 2014. Article (CrossRef Link)
[16] K. El Baamrani, V. P. Gil Jimenez, A. G. Armada, and A. A. Ouahman, "Multiuser Subcarrier and Power Allocation Algorithm for OFDM/Offset-QAM," *IEEE Signal Processing Letters*, vol. 17, no. 2, pp. 161-165, February, 2010. Article (CrossRef Link)
[17] P. Achaichia, M. L. Bot, P. Siohan, "OFDM/OQAM: A Solution to Efficiently Increase the Capacity of Future PLC Networks," *IEEE Transactions on Power Delivery*, vol. 26, no. 4, pp.2443-2455, October, 2011. Article (CrossRef Link)
[18] B. F. Boroujeny, "OFDM Versus Filter Bank Multicarrier," *IEEE Signal Processing Magazine*, vol. 28, no. 3, pp.92-112, May, 2011. Article (CrossRef Link)
[19] N. Michailow, M. Matthe, I. S. Gaspar, et al, "Generalized Frequency Division Multiplexing for 5th Generation Cellular Networks," *IEEE Transactions on Communications*, vol. 62, no. 9, pp. 3045-3061, September, 2014. Article (CrossRef Link)
[20] J. P. Javaudin, D. Lacroix and A. Rouxel, "Pilot-aided channel estimation for OFDM/OQAM," in *Proc. of the 57th IEEE Semiannual Vehicular Technology Conference*, pp.1581-1585, April 22-25, 2003. Article (CrossRef Link)
[21] C. Lele, J. P. Javaudin, R. Legouable, A. Skrzypczak and P. Siohan, "Channel estimation methods for preamble-based OFDM/OQAM modulations," *European Transactions on Telecommunications*, vol. 19, no. 7, pp.741-750, March 26-28, 2008. Article (CrossRef Link)
[22] J. F. Du, S. Signell, "Novel Preamble-Based Channel Estimation for OFDM/OQAM Systems," in *Proc. of IEEE International Conference on Communications*, pp.1-6, June 14-18, 2009. Article (CrossRef Link)
[23] E. Kofidis, D. Katselis. "Improved interference approximation method for preamble-based channel estimation in FBMC/OQAM," in *Proc. of the 19th European Signal Processing Conference (EUSIPCO 2011)*, pp.1603-1607, August 29- September 2, 2011. Article (CrossRef Link)
[24] S. W. Kang, K. H. Chang, "A novel channel estimation scheme for OFDM/OQAM-IOTA system," *ETRI Journal*, vol. 29, no. 4, pp.430-436, April, 2007. Article (CrossRef Link)
[25] B. Mongol, T. Yamazato, and M. Katayama, "Channel estimation and tracking schemes for the pulse-shaping OFDM systems," in *Proc. of IEEE International Conference on Communications*, June 14-18, 2009. Article (CrossRef Link)
[26] F. Deng, X. He, G.B. Cheng, S. Q. Li, "An effective Preamble-based Channel Estimation Structure for OFDM/OQAM Systems," in *Proc. of the 6th International Conference on Wireless Communications Networking and Mobile Computing*, pp.1-4, September 23-25, 2010. Article (CrossRef Link)

[27] S.Hu, G. Wu, T. Li, Y. Xiao, Q.S. Li, "Preamble design with ICI cancellation for channel estimation in OFDM/OQAM system," *IEICE Transactions on Communications*, vol. E93-B, no. 1, pp.211-214, January, 2010. Article (CrossRef Link)
[28] T. W. Yoon, S. Tm, S. H. Hwang, H. J. Choi, "Pilot Structure for High Data Rate in OFDM/OQAM-IOTA System," in *Proc. of the 68th IEEE Vehicular Technology Conference*, pp. 1-5, September 21-24, 2008. Article (CrossRef Link)
[29] C. Lele, P. Siohan, and R. Legouable, "2 dB better than CP-OFDM with OFDM/OQAM for preamble-based channel estimation," in *Proc. of IEEE International Conference on Communications*, pp. 1302-1306, May 19-23, 2008. Article (CrossRef Link)
[30] D. Katselis, E. Kofidis, "Preamble-Based Channel Estimation for CP-OFDM and OFDM/OQAM Systems: A Comparative Study," *IEEE Transactions on Signal Processing*, vol. 58, no. 5, pp. 2911-2917, May, 2010. Article (CrossRef Link)
[31] B. Zayani, H. Shaiek, D. Roviras, and Y. Medjahdi, "Closed-Form BER Expression for (QAM or OQAM)- Based OFDM System With HPA Nonlinearity Over Rayleigh Fading Channel," *IEEE Wireless Communications Letters*, vol. 4, no. 1, pp. 38-41, February, 2015. Article (CrossRef Link)

Han Wang received his B.S. degree in electrical engineering from Hubei University of Nationalities, China, in 2009 and the M.S. degree in information and communication system from Hainan University, Haikou, China, in 2013. He has worked in China Mobile Jiangxi branch as a network engineer for one year. Now, he is pursuing the Ph.D. degree with the Department of College of Information Science & Technology in Hainan University. His research interests include maritime communications and information theory.

Wencai Du received the B.S. degree from Peking University, China, two M.S. Degrees from ITC, The Netherlands, and Hohai University, China, respectively, and Ph.D. degree from South Australia University, Australia. He was a Post-doctor Fellow in Israel Institute of Technology (IIT), Haifa, Israel. He is Dean of College of Information Science & Technology at Hainan University and Director of Maritime Communication and Engineering of Hainan province. He has authored or coauthored 18 books and more than 80 scientific publications. His research interests include several aspects of Information Technology and Communication (ITC), including computer network and maritime communications.

Lingwei Xu was born in Shandong Province, China, in 1987. He received his M.E. degree in Electronics and Communication Engineering from Ocean University of China, in 2013 and his Ph.D. degree in Ocean University of China in June 2016. Now he is a lecturer in Qingdao University of Science& Technology. His research interests include ultra-wideband radio systems, MIMO wireless systems, and M2M wireless communications.